Stress Analysis in Platform-Switching Implants: A 3-Dimensional Finite Element Study

Eduardo Piza Pellizzer, DDS, PhD, MSc[1]*
Fellippo Ramos Verri, DDS, PhD, MSc[1]
Rosse Mary Falcón-Antenucci, DDS, MSc[1]
Joel Ferreira Santiago Júnior, DDS[1]
Paulo Sérgio Perri de Carvalho, DDS, PhD, MSc[2]
Sandra Lúcia Dantas de Moraes, DDS, MSc[1]
Pedro Yoshito Noritomi, PhD, MSc[3]

The aim of this study was to evaluate the influence of the platform-switching technique on stress distribution in implant, abutment, and peri-implant tissues, through a 3-dimensional finite element study. Three 3-dimensional mandibular models were fabricated using the SolidWorks 2006 and InVesalius software. Each model was composed of a bone block with one implant 10 mm long and of different diameters (3.75 and 5.00 mm). The UCLA abutments also ranged in diameter from 5.00 mm to 4.1 mm. After obtaining the geometries, the models were transferred to the software FEMAP 10.0 for pre- and postprocessing of finite elements to generate the mesh, loading, and boundary conditions. A total load of 200 N was applied in axial (0°), oblique (45°), and lateral (90°) directions. The models were solved by the software NeiNastran 9.0 and transferred to the software FEMAP 10.0 to obtain the results that were visualized through von Mises and maximum principal stress maps. Model A (implants with 3.75 mm/abutment with 4.1 mm) exhibited the highest area of stress concentration with all loadings (axial, oblique, and lateral) for the implant and the abutment. All models presented the stress areas at the abutment level and at the implant/abutment interface. Models B (implant with 5.0 mm/abutment with 5.0 mm) and C (implant with 5.0 mm/abutment with 4.1 mm) presented minor areas of stress concentration and similar distribution pattern. For the cortical bone, low stress concentration was observed in the peri-implant region for models B and C in comparison to model A. The trabecular bone exhibited low stress that was well distributed in models B and C. Model A presented the highest stress concentration. Model B exhibited better stress distribution. There was no significant difference between the large-diameter implants (models B and C).

INTRODUCTION

Bone remodeling surrounding osseointegrated implants has been used for decades as a parameter to assess the predictability of prosthetic rehabilitation.[1] Bone loss of 1.5 mm during the first year of loading and 0.1 mm in the subsequent years is considered acceptable.[1–3] Recently, the platform-switching technique has decreased the possibility of bone loss in the peri-implant region.[4–11]

The platform-switching technique consists of using an implant with a large diameter and an abutment with small diameter. The resorption pattern was not exhibited in patients with the platform-switching technique after a 5-year follow-up according to radiographic examinations.[12] Lazzara and Porter[12] stated that this phenomenon occurs because of the displacement of the implant-abutment junction to the central axis of the implant and transferring of microgap at the implant-abutment interface that may exhibit bacterial leakage, which avoids inflammation in the bone crest.

Clinical, retrospective, and histomorphometric studies demonstrated preservation of bone ridge

[1] Department of Dental Materials and Prosthodontics, Araçatuba School of Dentistry, São Paulo State University-UNESP, Brazil.
[2] Department of Surgery and Integrated Clinic, Araçatuba School of Dentistry, São Paulo State University-UNESP, Brazil.
[3] Renato Archer Information Technology Center, São Paulo, Brazil.
* *Corresponding author,* e-mail: ed.pl@uol.com.br
DOI: 10.1563/AAID-JOI-D-10-00041

Table 1
Models of the study

Model	Description
A	External hexagon implants with 5.00/UCLA with 4.1-mm diameter
B	External hexagon implants with 5.00/UCLA with 5.0-mm diameter
C	External hexagon implants with 5.00/UCLA with 4.1-mm diameter

Table 2
Material properties

Material	Elastic Modulus (MPa)	Poisson's Coefficient (μ)	Reference
Trabecular bone	1.370	0.30	Sertgöz[16]
Cortical bone	13.700	0.30	Sertgöz[16]
Titanium (implant abutment)	110.000	0.35	Sertgöz[16]

or reduced bone loss surrounding these implants.[4–6,9,10] Recent research focused on the biomechanics of the platform-switching technique using different methodologies suggested displacement of stress to the long axis of the implant with stress concentration at the abutment-implant interface that was reduced in the peri-implant region.[13–15]

The stability of the peri-implant bone level after loading is an important factor for rehabilitation success. Thus, it is relevant to evaluate if the alteration of traditional abutment-implant connection design (platform-switching technique) may improve the stress distribution from abutment to implant and from implant to bone. Recent studies demonstrated that increased diameter[15–18] is a predominant factor for stress reduction with platform switching. Hence, the evaluation of real biomechanical benefits of the reduced abutment platform attached to the implants still remains inconclusive. The hypothesis of the present study states that stress in bone is reduced with increased implant diameter according to the platform-switching technique. Therefore, the aim of this study is to evaluate the biomechanical advantages of platform-switching implants regarding stress distribution on implant, abutment, and peri-implant regions in comparison with implants with regular (3.75 mm) and large (5.00 mm) diameters.

Materials and Methods

Three models were fabricated. Each model represented a bone block (cortical and trabecular) of the mandibular molar region with one external hexagon implant with a length of 10 mm (Master Screw, Conexão Sistema de Prótese Ltda, São Paulo, Brazil) and different diameters (3.75 and 5.00 mm). The diameter of the titanium UCLA abutment also ranged from 4.1 to 5.0 mm. Table 1 illustrates the specifications of each model.

The trabecular and cortical bone were represented according to a computerized tomography of the transversal section in the molar region transferred to the software InVesalius (CTI Renato Archer, São Paulo, Brazil) that creates 3-dimensional virtual models using the transversal slices of tomography.

The geometries of the external hexagon implants and the UCLA abutment were used as a reference to fabricate the model. These components were simulated by the design software SolidWorks 2006 (SolidWorks Corp, Concord, Mass). After fabrication of the models, the geometries were transferred to the software of pre- and postprocessing of finite elements, FEMAP 10.0 (Siemens PLM Software Inc, Santa Ana, Calif) in STEP format. Thus, the finite element meshes were generated with parabolic solid elements.

The mechanical properties of each material were incorporated, such as elastic modulus and Poisson's coefficient, according to the values obtained in the literature,[16] as shown in Table 2. All materials were considered isotropic, linearly elastic, and homogeneous.

The model was defined according to the boundary and loading conditions. The bone block was fixed in the 3 axes in the lateral faces, the base was considered free or suspended, and the implant was considered osseointegrated. The total load in the model was 200 N[17] in the axial, oblique (45°), and lateral direction distributed into 4 points on the abutment surface.

Then, the analysis was generated in the software of pre- and postprocessing of finite elements FEMAP 10.0 and transferred for calculation in the software NeiNastran version 9.2 (Noran Engineering, Inc, Westminster, Calif). The procedures were conducted in a workstation (Sun Microsystems Inc, São Paulo, Brazil). The results were transferred to

the software FEMAP 10.0 for visualization and postprocessing of the von Mises and maximum principal stress maps.

Results

Von Mises stress

General Map

According to a sagittal slice, it was observed that the models under axial loading presented the lowest stress on abutment and implant-abutment interface. However, for lateral (Figure 1) and oblique loading, stress was exhibited on abutment, implant-abutment interface, and implant threads with low intensity on the apical third.

The comparative analysis revealed the highest area of stress concentration in the model A (16.25–130 MPa) with lateral loading (Figure 1A).

Implant

All models exhibited low concentrations with axial load, and model C presented the highest stress concentration at the platform of about 12.19–28.13 MPa. For oblique and lateral loads, stress was concentrated at the platform and the cervical-medium third (threads) of the implant in all models.

The comparative analysis revealed the highest area of stress concentration with lateral loading, and model C exhibited the highest stress (12.5–93.75 MPa).

Abutment

The highest stress was concentrated at the medium and coronal thirds of the abutment in the 3 models under loading (axial, oblique, and lateral). The stress distribution pattern was similar for oblique and lateral loading.

The comparative analysis revealed that model C (20.31–130 MPa) presented the highest area of stress concentration under lateral loading and the lowest area under axial loading (8.125–32.5 MPa; Figures 2–4).

Maximum principal stress

Cortical Bone

The stress distribution pattern was similar for axial, oblique, and lateral loading (Figure 5). The stress was concentrated surrounding the collar and the first thread of the implant (Figures 6–8).

The comparative analysis demonstrated that model A presented the highest stress concentration under axial, oblique, and lateral loading (−5.625 to 15 MPa). Model B exhibited the best stress distribution under axial and oblique loading.

Trabecular Bone

The models are represented in Figures 9, 10, and 11. The stress distribution pattern was similar for axial and oblique loading (Figures 9 and 10). Stress was distributed surrounding the implant body, and the highest stress was concentrated at the first thread. However, for the load direction, model C presented the highest stress area between the platform and the first thread in comparison with model B.

The comparative analysis revealed that the model A presented the highest stress concentration under axial (−0.25 to 1.5 MPa), oblique (−0.375 to 1.5 MPa), and lateral (−0.438 to 1.5 MPa) loading. The lowest stress was exhibited in the model C (−0.25 to 1.125 MPa).

Discussion

In the present study, the analysis of the models (model A, regular diameter; model B, large diameter; and model C, platform switching) revealed that an increase in diameter (models B and C) was favorable for stress distribution, which is in agreement with studies that demonstrated that increased diameter favorably modulates the stress distribution.[14,15,18,19] According to Jarvis,[20] the large-diameter implant provides a major contact surface at the bone-implant interface that allows uniform load distribution and reduces stress surrounding the implant neck.

There was no significant difference for the comparison between models B and C, but model B exhibited more favorable situations in some cases. This fact probably results from the greatest contact area at the implant-abutment interface that allowed better stress distribution.

Comparing models B and C, the platform-switching model (model C) presented a higher stress area (12.5–93.75 MPa) probably because of a minor contact area at the implant-abutment interface, which generated the highest stress concentration in this area that also reflects on the implant. This highest concentration on the abutment in the platform-switching model is in accordance with the

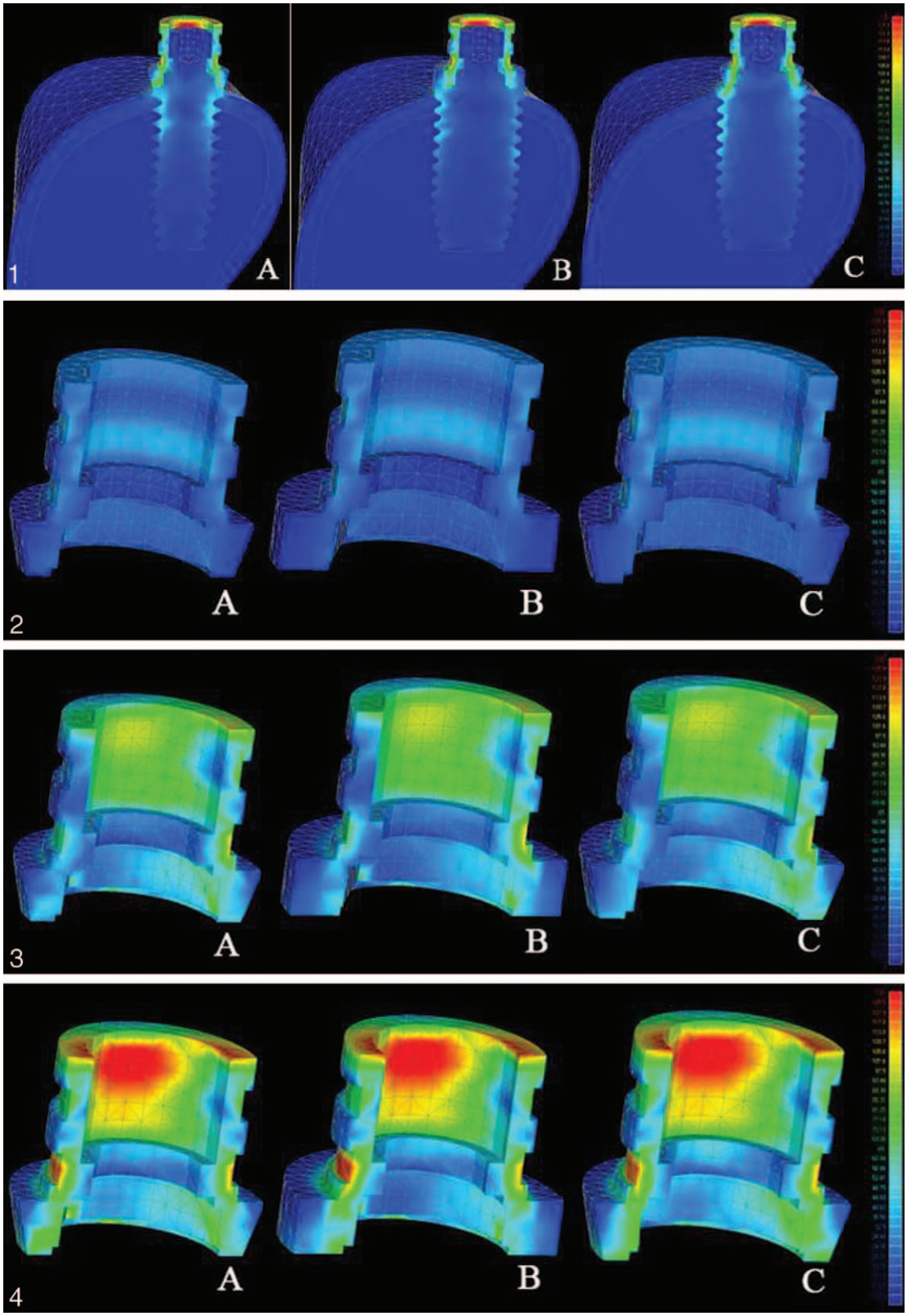

Figures 1–4. Figure 1. Von Mises general map: lateral load. **Figure 2.** Von Mises stress maps: abutment, axial load. **Figure 3.** Von Mises stress maps: abutment, oblique load. **Figure 4.** Von Mises stress maps: abutment, lateral load.

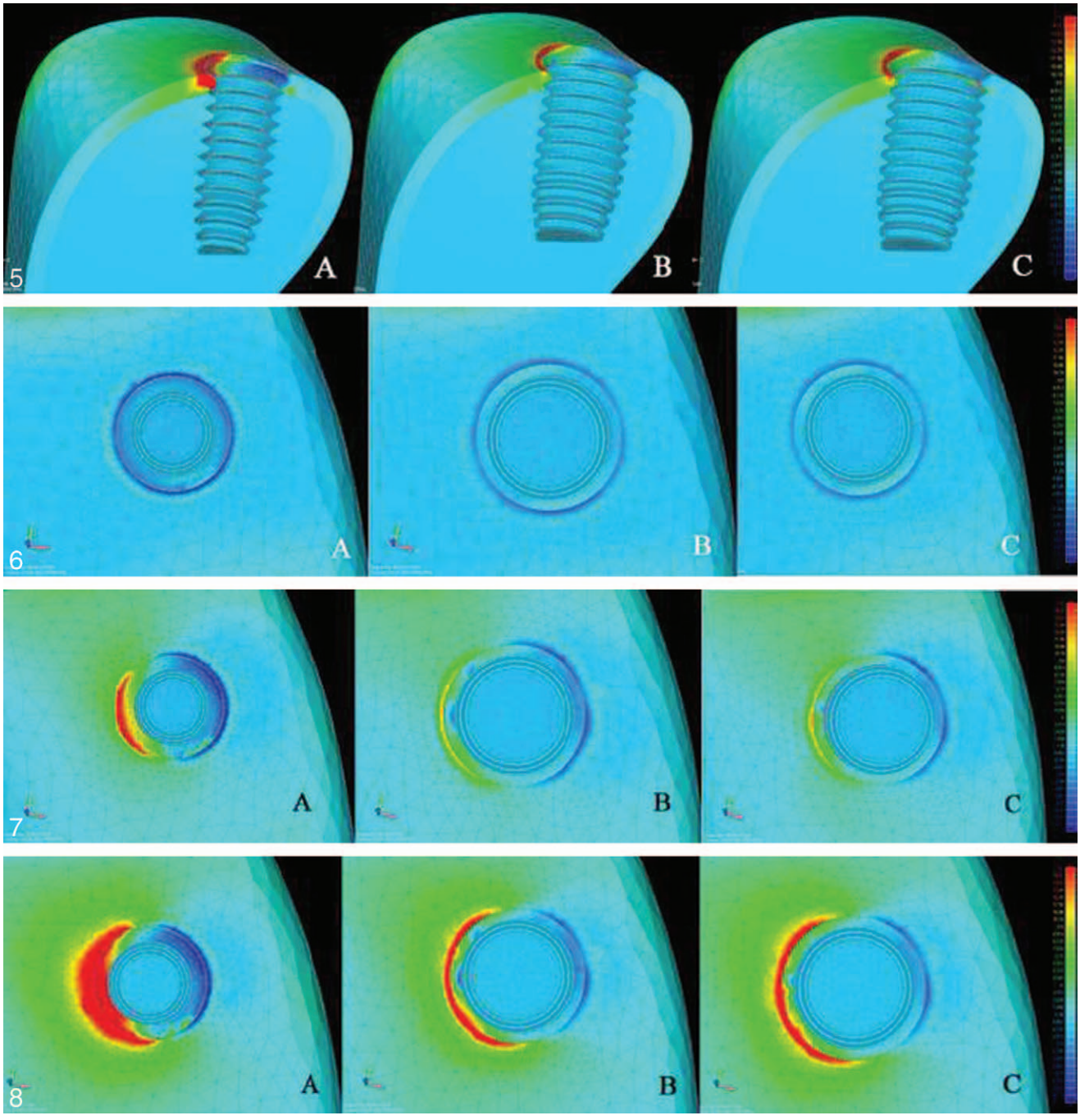

Figures 5–8. Figure 5. Von Mises stress maps: cortical and trabecular bone, lateral load. **Figure 6.** Von Mises stress maps: cortical bone, axial load. **Figure 7.** Von Mises stress maps: cortical bone, oblique load. **Figure 8.** Von Mises stress maps: cortical bone, lateral load.

results obtained by Maeda et al,[14] which reported the probability of abutment screw failure due to the highest stress concentration in this area, which may not be clinically relevant.

Considering the stress in the cortical bone, model A exhibited the highest value (implant with 3.75 mm) that was exhibited in the first threads. Similarly to other studies,[21–23] cortical bone presents an elastic modulus about 7 to 10 times higher than trabecular bone. Thus, the cortical bone acts like a fulcrum when transversal loads are applied.[24] Cortical bone also concentrates the highest stress in comparison with trabecular bone because of higher rigidity.[25] In models B and C, the

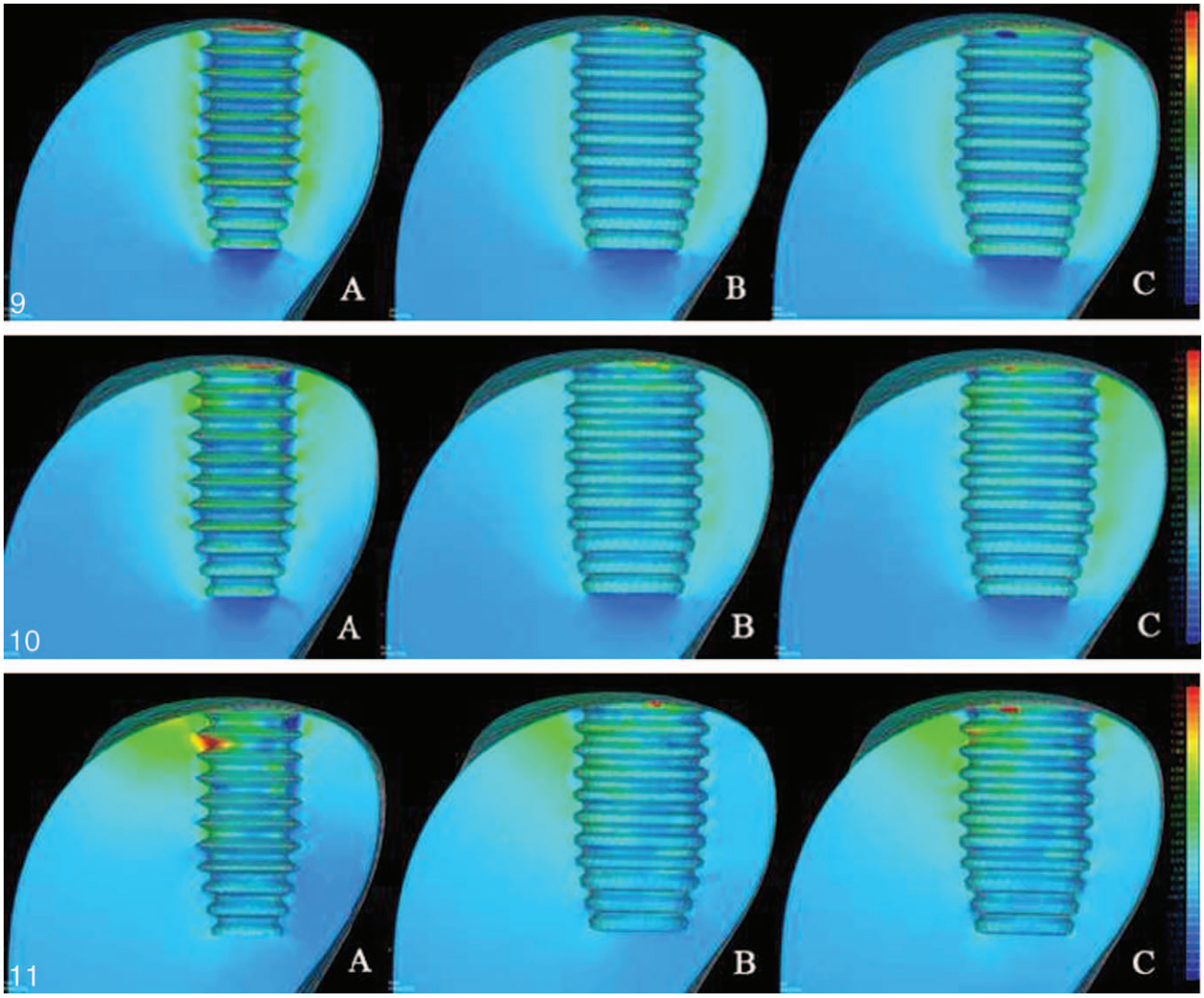

Figures 9–11. Figure 9. Von Mises stress maps: trabecular bone, axial load. **Figure 10.** Von Mises stress maps: trabecular bone, oblique load. **Figure 11.** Von Mises stress maps: trabecular bone, lateral load.

areas of compression and traction stress were minor, and the values (−5.625 to 12.94 MPa) were within the physiological limits reported in the literature of 170 MPa for compression and 100 MPa for traction.[26]

In the present study, the use of a large-diameter model (model B) demonstrated that not always does an increase in implant diameter lead to stress reduction. There was no significant difference between models B and C, as was also observed by Schrotenboer et al[27] using 2D finite element analysis. These authors concluded that the reduction in abutment diameter presented a minimum effect on cortical bone when comparing 2 large-diameter implants and different abutment sizes. Similar results were found by Pellizzer et al[13] through photoelasticity, concluding that models A (platform switching) and C (conventional/large-diameter) exhibited similar stress intensity. Considering the loads, the horizontal component (lateral load) revealed higher stress in all models, as it was also demonstrated by other studies[28,29] that reported the highest stress concentration with lateral loads.

Hsu et al[15] conducted a 3D finite element analysis with similar conditions to the present study and concluded that stress in bone was reduced by increased implant diameter rather than by the platform-switching technique. However, Tabata et al[30] arrived at conclusions that contradicted those of the previously mentioned authors when using a 2D finite element analysis.

They proposed a model with 4.0-mm implants with a 4.1-mm platform and 4.1-mm abutment; the platform-switching model was a 5.0-mm implant with a 5.0-mm platform and a 4.1-mm abutment, and the authors concluded that platform switching was more favorable. In our view, the factor that allowed better stress distribution was not the platform-switching implant technique but the increased diameter of the implant.

The platform-switching technique is biomechanically explained considering that the stress distribution on this implant (model C) was relatively similar to the large-diameter implant and abutment in model B.[15,18] Hence, it is suggested that the greatest benefits of this technique are related to the preservation of the bone ridge due to the biological benefit[13] and distance between the microgap-induced inflammation and the bone ridge, which allows for a more favorable remodeling in comparison with the large-diameter implant abutment.

Thus, platform-switching implants are a reliable and satisfactory alternative for biomechanics and a simple and low-cost technique. The biological benefits[3–6,8,10] justify its application since there was no significant difference for its counterindication. However, further longitudinal and biomechanical studies are required.

Conclusion

According to the methodology, we concluded the following:

- Model A (implant with 3.75-mm/abutment with 4.1 mm) presented the highest stress concentration. Model B (implant with 5.00-mm/abutment with 5.00 mm) exhibited better stress distribution.
- There was no significant difference between the large-diameter implants (models B and C).

References

1. Smith DE, Zarb GA. Criteria for success of osseointegrated endosseous implants. *J Prosthet Dent*. 1989;62:567–572.

2. Albrektsson T, Zarb G, Worthington P, Eriksson AR. The long-term efficacy of currently used dental implants: a review and proposed criteria of success. *Int J Oral Maxillofac Implants*. 1986;1: 11–25.

3. Hermann JS, Buser D, Schenk RK, et al. Biologic width around titanium implants: a physiologically formed and stable dimension over time. *Clin Oral Implants Res*. 2000;11:1–11.

4. Calvo Guirado JL, Saez Yuguero MR, Pardo Zamora G, et al. Immediate provisionalization on a new implant design for esthetic restoration and preserving crestal bone. *Implant Dent*. 2007;16:155–164.

5. Gardner DM. Platform switching as a means to achieving implant esthetics. *N Y State Dent J*. 2005;71:34–37.

6. Baumgarten H, Cocchetto R, Testori T, et al. A new implant design for crestal bone preservation: initial observations and case report. *Pract Periodont Aesthet Dent*. 2005;17:735–740.

7. Canullo L, Rasperini G. Preservation of peri-implant soft and hard tissues using platform switching of implants placed in immediate extraction sockets: a proof-of-concept study with 12- to 36-month follow-up. *Int J Oral Maxillofac Implants*. 2007;22:995–1000.

8. Calvo Guirado JL, Ortiz Ruiz AJ, Gómez Moreno G, et al. Immediate loading and immediate restoration in 105 expanded-platform implants via the Diem System after a 16-month follow-up period. *Med Oral Patol Oral Cir Bucal*. 2008;13:E576–E581.

9. Vela-Nebot X, Rodríguez-Ciurana X, Rodado-Alonso C, Segalà-Torres M. Benefits of an implant platform modification technique to reduce crestal bone resorption. *Implant Dent*. 2006;15: 313–320.

10. Hürzeler M, Fickl S, Zuhr O, Wachtel HC. Peri-implant bone level around implants with platform-switched abutments: preliminary data from a prospective study. *J Oral Maxillofac Surg*. 2007;65: 33–39.

11. Cappiello M, Luongo R, Di Iorio D, Bugea C, Cocchetto R, Celletti R. Evaluation of peri-implant bone loss around platform-switched implants. *Int J Periodontics Restorative Dent*. 2008;28:347–355.

12. Lazzara RJ, Porter SS. Platform switching: a new concept in implant dentistry for controlling postrestorative crestal bone levels. *Int J Periodontics Restorative Dent*. 2006;26:9–17.

13. Pellizzer EP, Falcón-Antenucci RM, Carvalho PSP, Santiago JF Jr, Moraes SLD, Carvalho BM. Photoelastic analysis of the influence of platform switching on stress distribution in implants. *J Oral Implantol*. 2010;36:419–424.

14. Maeda Y, Miura J, Taki I, Sogo M. Biomechanical analysis on platform switching: is there any biomechanical rationale?. *Clin Oral Implants Res*. 2007;18:581–584.

15. Hsu JT, Fuh LJ, Lin DJ, Shen YW, Huang HL. Bone strain and interfacial sliding analyses of platform switching and implant diameter on an immediately loaded implant: experimental and three-dimensional finite element analyses. *J Periodontol*. 2009;80: 1125–1132.

16. Sertgöz A. Finite element analysis study of the effect of superstructure material on stress distribution in an implant-supported fixed prosthesis. *Int J Prosthodont*. 1997;10:19–27.

17. Morneburg TR, Pröschel PA. Measurement of masticatory forces and implant loads: a methodologic clinical study. *Int J Prosthodont*. 2002;15:20–27.

18. Schrotenboer J, Tsao YP, Kinariwala V, Wang HL. Effect of microthreads and platform switching on crestal bone stress levels: a finite element analysis. *J Periodontol*. 2008;79:2166–2172.

19. Himmlová L, Dostálová T, Kácovský A, Konvicková S. Influence of implant length and diameter on stress distribution: a finite element analysis. *J Prosthet Dent*. 2004;91:20–25.

20. Jarvis WC. Biomechanical advantages of wide-diameter implants. *Compend Contin Educ Dent*. 1997;18:687–692.

21. Liu XJ, Li ZY, Xia HB. Influence of implant-abutment connection mode on stress distribution in peri-implant bone. *Zhonghua Kou Qiang Yi Xue Za Zhi*. 2008;43:50–53.

22. Weinberg LA. The biomechanics of force distribution in

implant-supported prostheses. *Int J Oral Maxillofac Implants*. 1993; 8:19–31.

23. Rangert B, Jemt T, Jörneus L. Forces and moments on Branemark implants. *Int J Oral Maxillofac Implants*. 1989;4:241–217.

24. Rodríguez-Ciurana X, Vela-Nebot X, Segalà-Torres M, et al. Biomechanical repercussions of bone resorption related to biologic width: a finite element analysis of three implant-abutment configurations. *Int J Periodontics Restorative Dent*. 2009;29:479–487.

25. Koca OL, Eskitascioglu G, Usumez A. Three-dimensional finite-element analysis of functional stresses in different bone locations produced by implants placed in the maxillary posterior region of the sinus floor. *J Prosthet Dent*. 2005;93:38–44.

26. Martin RJ, Goupil MT, Goldschmidt M. Single-implant segmental osteotomy: a case report. *Int J Oral Maxillofac Implants*. 1998;13:710–712.

27. Schrotenboer J, Tsao YP, Kinariwala V, Wang HL. Effect of platform switching on implant crest bone stress: a finite element analysis. *Implant Dent*. 2009;18:260–269.

28. Sütpideler M, Eckert SE, Zobitz M, An KN. Finite element analysis of effect of prosthesis height, angle of force application, and implant offset on supporting bone. *Int J Oral Maxillofac Implants*. 2004;19:819–825.

29. Holmgren EP, Seckinger RJ, Kilgren LM, et al. Evaluating parameters of osseointegrated dental implants using finite analysis-a two-dimensional comparative study examining the effects of implant diameter, implant shape, and load direction. *J Oral Implantol*. 1998;24:80–88.

30. Tabata LF, Assunção WG, Barão VAR, Souza EAC, Gomes EA, Delben JA. Implant platform switching: biomechanical approach using two-dimensional finite element analysis. *J Craniofac Surg*. 2010;21:182–187.